Journal of Photochemistry and Photobiology A: Chemistry 214 (2010) 54–60

Contents lists available at ScienceDirect

Journal of Photochemistry and Photobiology A: Chemistry

journal homepage: www.elsevier.com/locate/jphotochem

Flux synthesis of $AgNbO_3$: Effect of particle surfaces and sizes on photocatalytic activity

David Arney, Christopher Hardy, Benjamin Greve, Paul A. Maggard*

Department of Chemistry, North Carolina State University, Raleigh, NC 27695-8204, United States of America

ARTICLE INFO

Article history:
Received 6 December 2009
Received in revised form 3 June 2010
Accepted 7 June 2010
Available online 15 June 2010

Keywords:
Flux synthesis
$AgNbO_3$
Photocatalysis

ABSTRACT

The molten-salt flux synthesis of $AgNbO_3$ particles was performed in a Na_2SO_4 flux using 1:1, 2:1 and 3:1 flux-to-reactant molar ratios and heating to 900 °C for reaction times of 1–10 h. Rectangular-shaped particles are obtained in high purity and with homogeneous microstructures that range in size from ~100 to 5000 nm and with total surface areas from 0.16 to 0.65 $m^2\ g^{-1}$. The smallest particle-size distributions and highest surface areas were obtained for the largest amounts of flux (3:1 ratio) and the shortest reaction time (1 h). Measured optical bandgap sizes of the $AgNbO_3$ products were in the range of ~2.8 eV. The photocatalytic activities of the $AgNbO_3$ particles for H_2 formation were measured in visible light ($\lambda > 420$ nm) in an aqueous methanol solution and varied from ~1.7 to 5.9 $\mu mol\ H_2\ g^{-1}\ h^{-1}$. The surface microstructures of the particles were evaluated using field-emission SEM, and the highest photocatalytic rates of the $AgNbO_3$ particles were correlated with the formation of high densities of ~20–50 nm terraced surfaces. By comparison, the solid-state sample showed no well-defined morphology or microstructure. Thus, the results presented herein demonstrate the utility of flux-synthetic methods in targeting new particles sizes and surface microstructures for the enhancement and understanding of photocatalytic reactivity over metal-oxide particles.

1. Introduction

Photocatalytic hydrogen production from solar energy and water using metal-oxide particles is a rapidly expanding field of renewable energy research [1–4]. Numerous metal oxides have been shown to split water into hydrogen and oxygen in aqueous solutions when irradiated by high-energy ultraviolet photons, including $NaTaO_3$ [5], $Sr_2Nb_2O_7$ [6,7], $La_2Ti_2O_7$ [8], as well as many others [9–16]. However, the highest intensities and greatest fraction (>50%) of the solar spectrum consist of visible-light wavelengths, and thus the synthesis of new photocatalysts that efficiently utilize visible-light photons for hydrogen production could help realize significant new technological advancements. Previously, it has been shown that Ag^+-containing early transition-metal oxides can absorb light out to the visible wavelengths owing to their smaller bandgap sizes [17–19]. This arises because of the higher-energy valence band that derives from the filled Ag 4d orbitals, and which is still sufficiently below the (O_2/H_2O) oxidation potential. Previous studies on $AgNbO_3$ and $AgTaO_3$ have shown that their bandgap sizes are ~2.8 eV and ~3.4 eV [17], respectively, and that the photon-driven oxidation and reduction of water is feasible in visible light using suitable sacrificial reagents. $AgTaO_3$ is reportedly inactive for the photocatalytic production of H_2 in visible light owing to its larger bandgap size, but $AgNbO_3$ was found to be active in visible light using sacrificial reagents with low rates of ~1.5 $\mu mol\ H_2\ g^{-1}\ h^{-1}$ [17]. However, the synthesis of $AgNbO_3$ and $AgTaO_3$ in these photocatalysis studies proceeded via traditional solid-state methods. This synthetic route provides almost no control over the particle sizes and/or surface characteristics of the metal-oxide particles where the photon-initiated oxidation and reduction reactions occur (i.e. the active sites of the reaction). Utilization of new synthetic methods to better gain control over the particle features of metal oxides can potentially enable a deeper understanding of these reactions. As an alternative synthetic method, the use of molten-salt flux techniques for the preparation of metal oxides can enable shorter reaction times, reduced reaction temperatures, and tunability of the particle features, such as their sizes and morphologies [20–25,30–33].

Thus, new synthetic investigations into the preparation of $AgNbO_3$ particles by flux-synthetic techniques were conducted in order to determine the roles the particle sizes and surfaces had in the photocatalytic activities. The flux synthesis of large single crystals of $AgNbO_3$ for X-ray analysis has been reported previously in the literature based on the use of AgCl and Ag_2SO_4 fluxes [26,27].

* Corresponding author at: Department of Chemistry, North Carolina State University, 2620 Yarbrough Drive, 740 Dabney Hall, Raleigh, NC 27695-8204, United States of America. Tel.: +1 919 515 3616; fax: +1 919 515 5079.
E-mail address: Paul_Maggard@ncsu.edu (P.A. Maggard).

1010-6030/$ – see front matter © 2010 Elsevier B.V. All rights reserved.
doi:10.1016/j.jphotochem.2010.06.006

However, the research motivation herein was to investigate flux-synthetic routes to much smaller particle sizes of $AgNbO_3$, and to compare the resultant photocatalytic activities, surface areas, and particles sizes with those products obtained from traditional solid-state methods. Described herein is the synthesis of $AgNbO_3$ particles within a molten Na_2SO_4 flux, and an investigation of the effects of reaction durations and flux-to-reactant ratios on the particle sizes and morphologies, as well as their optical properties and photocatalytic rates for H_2 formation. The products were characterized by powder X-ray diffraction, UV–vis diffuse reflectance spectroscopy, BET surface area analysis, field-emission scanning electron microscopy, and their visible-light photocatalytic activities for H_2 production.

2. Experimental

2.1. Synthesis and characterization

The flux synthesis of $AgNbO_3$ was performed by combining a well-ground stoichiometric mixture of Ag_2O and Nb_2O_5 and adding this to a Na_2SO_4 salt flux to give flux-to-reactant molar ratios of 1:1, 2:1, and 3:1. The reactant mixtures were then placed inside an alumina crucible and heated to 900 °C inside a box furnace for reaction times of 1, 2, and 10 h. The crucibles were allowed to radiatively cool to room temperature inside the furnace. Additionally, 1:1 flux-prepared samples were slow cooled to 750 °C at rates of 15 °C/h and 3 °C/h, respectively, before then radiatively cooling to room temperature. The resulting products were washed with hot deionized water to remove the flux, and then briefly washed once with 1 M HNO_3 to remove any excess silver and dried overnight in an oven at 80 °C. A fine homogeneous grayish powder of $AgNbO_3$ was obtained in high purity, as judged from powder X-ray diffraction. The solid-state method of preparing $AgNbO_3$ involved grinding, pelletizing, and heating the Ag_2O and Nb_2O_5 reactants to 900 °C for 12 h, according to the reported procedures [17].

High-resolution powder X-ray diffraction (PXRD) data of all products were collected on an INEL diffractometer using Cu $K\alpha_1$ (λ = 1.54056 Å) radiation from a sealed-tube X-ray generator (35 kV, 30 mA) using a curved position sensitive detector (CPS120). Unit-cell parameters of the flux-prepared samples were calculated using the LATCON software [28]. Field-emission scanning electron microscopy analyses were performed on a JEOL SEM 6400, and concomitantly the energy dispersive X-ray (EDX) spectra were taken as a check of the elemental compositions. UV–vis diffuse reflectance spectra (DRS) were collected for all samples on a Shimadzu UV-3600 spectrophotometer equipped with an integrating sphere. BET surface area analyses were performed using a Quantachrome ChemBET Pulsar TPR/TPD.

2.2. Photocatalysis testing

The photocatalytic activity for H_2 formation was measured using an outer-irradiation type fused-silica reaction cell with a volume of 90 mL and irradiated under visible light (λ > 420 nm). First, each sample was loaded with a 1 wt% Pt cocatalyst using the photodeposition method [5]. Numerous previous studies have shown that platinum islands on a metal oxide surface can function as a kinetic aid to the reduction of H_2O to give H_2 [29]. Typically, 250 mg of a $AgNbO_3$ sample was mixed with 30 mL of an aqueous solution of dihydrogen hexachloroplatinate(IV) ($H_2PtCl_6{\cdot}6H_2O$; Alfa Aesar, 99.95%), and which was then irradiated for 6 h using a 400 W Xe arc-lamp with constant stirring using a magnetic stir bar. UV–vis measurements of the remaining solution confirmed a complete deposition of the platinum cocatalyst. After platinization, the particles were separated via centrifugation, washed with distilled water to remove any remaining Cl^- ions, and then dried overnight in an oven at 80 °C. For the photocatalytic H_2 measurements, the platinized $AgNbO_3$ was then added to the fused-silica reaction vessel that was filled with a 20% aqueous methanol solution. The added methanol functions as a hole scavenger, thereby generating CO_2 from its photo-oxidation, and which allows the measurement of the H_2 formation rate alone without the typically more difficult concomitant formation of O_2 being necessary and potentially rate limiting [4]. The net balanced reaction is: $CH_3OH + H_2O \rightarrow 3H_2 + CO_2$. The $AgNbO_3$ particles were first stirred in the dark for ~1–2 h, in order to remove any trapped gases on the particles' surfaces. Next, the reaction cell was irradiated under constant stirring for 6–12 h using an external 400 W Xe arc-lamp equipped with a long-pass cutoff filter (>420 nm), an IR water filter, and cooled using an external fan. The outlet of the photoreaction vessel was connected to a small horizontal quartz tube that trapped the evolved gases, and contained a moveable liquid bubble that allowed a volumetric determination of the amount of evolved gases at a constant pressure. The most active $AgNbO_3$ samples exhibited the formation of copious amounts of gases that rose to the top of the reaction cell, and that was observed to be consistent with the movement of the liquid bubble. The progress of the photocatalytic reactions was marked every hour and used to calculate the amount of gases generated in $\mu mol\, H_2\, g^{-1}\, h^{-1}$. The trapped gases were manually injected into a gas chromatograph (SRI MG #2; helium ionization and thermal conductivity detectors) in order to confirm the generated gases as H_2 and CO_2.

3. Results and discussion

3.1. Particle crystallinity, sizes, and surfaces

The $AgNbO_3$ particles crystallize in a perovskite-related structure in the orthorhombic space group P*bcm* [26]. The NbO_6 octahedra are condensed via corner sharing while Ag atoms occupy the interstitial sites, shown in Fig. 1. The Na_2SO_4 salt was chosen as a flux based on its previously successful use in the synthesis of La-doped $NaTaO_3$ and $La_2Ti_2O_7$ [30,31], as well as for its low cost and ease of removal after synthesis. The powder X-ray diffraction (PXRD) patterns of the flux-prepared $AgNbO_3$ products could be fitted and indexed to the reported structure type, as shown in Fig. 2 [27]. Refined unit-cell parameters for all samples are provided in Supporting Information. These PXRD data show that high purity and good crystallinity could be obtained in short reaction times of 1, 2, and 10 h and at Na_2SO_4 (flux):$AgNbO_3$ molar ratios of 1:1, 2:1 and 3:1. Synthetic attempts using larger flux:$AgNbO_3$ ratios and higher reaction temperatures resulted in the formation of $NaNbO_3$, as identified by PXRD. A barely detectable amount of $NaNbO_3$ was also observed as a separate phase in the PXRD patterns for the reactions at the 3:1 molar ratio. However, $NaNbO_3$ can be ruled out as a contributor to visible-light photocatalysis because of its large bandgap size (~3.4 eV), as reported previously [1].

In order to evaluate the $AgNbO_3$ particle sizes and morphologies, field-emission SEM images were taken on samples prepared using flux:$AgNbO_3$ ratios and heating times of 1:1 for 1 h (ANO1), 1:1 for 10 h (ANO3), 2:1 for 10 h (ANO6), 3:1 for 1 h (ANO7), 3:1 for 10 h (ANO9), and the solid-state prepared sample. These $AgNbO_3$ samples represent those having both the shortest and longest reaction times, and the smallest and largest amounts of flux used in the reaction. Shown in Fig. 3, the $AgNbO_3$ particles formed in rectangular and block-like shapes that clustered into larger aggregates of particles. A distribution of particle sizes was observed, with the edge dimensions of the particles typically ranging between ~100 and 700 nm for shorter reaction times of 1 h, and ~600–4000 nm for longer reaction times of 10 h. The amount of flux had a rela-

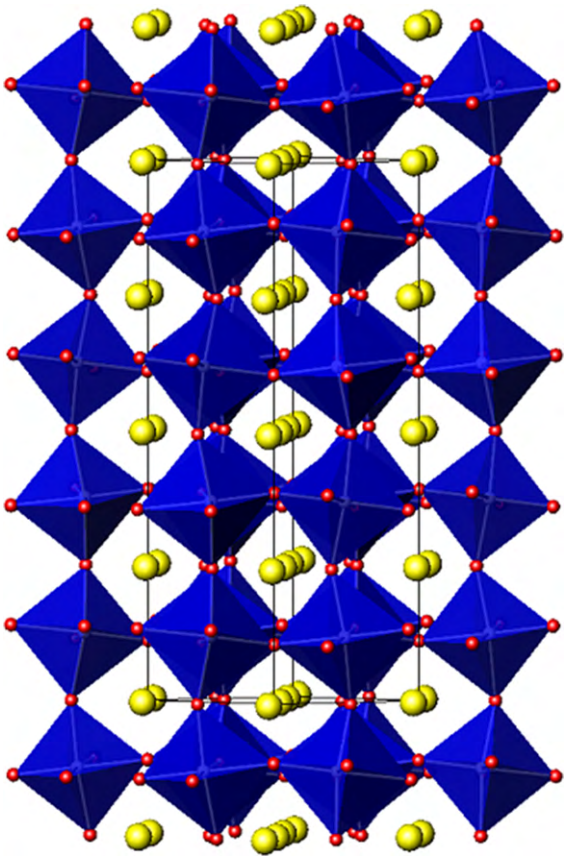

Fig. 1. Structure of $AgNbO_3$ with the unit-cell outlined; NbO_6 octahedra are blue, Ag atoms are yellow, and O atoms are red. (For interpretation of the references to color in this figure legend, the reader is referred to the web version of the article.)

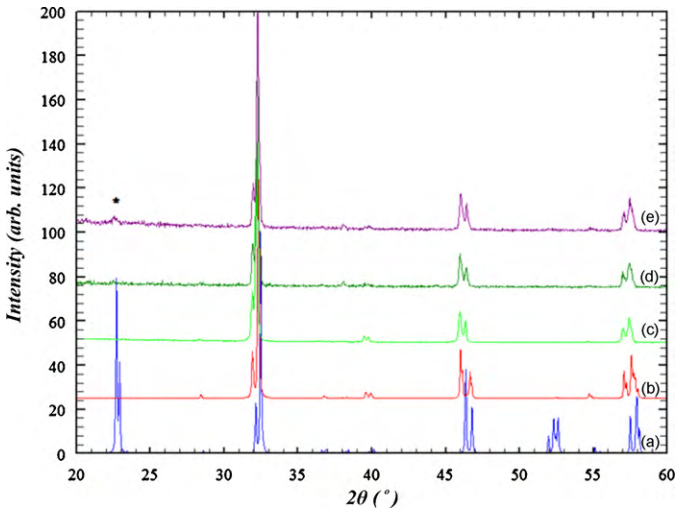

Fig. 2. Calculated PXRD patterns for $NaNbO_3$ (a) and $AgNbO_3$ (b), and the experimental PXRD patterns for $AgNbO_3$ prepared by the solid-state method (c) and using a 1:1 flux at 10 h (d; ANO3) and a 3:1 flux at 10 h (e; ANO9).

tively small effect on the $AgNbO_3$ particle sizes, as the particles prepared using larger amounts of flux were only a little smaller. An estimation of the average particle sizes was made based on size measurements on ~20 randomly selected particles that were observed in different regions of the sample. These measurements for the 1:1 flux:$AgNbO_3$ ratio, shown in Fig. 3A and B, yield average sizes of ~450 nm and ~1700 nm for the 1 h and 10 h reaction times, respectively. For the 3:1 flux:$AgNbO_3$ ratio, shown in Fig. 3C and D, average particle sizes of ~400 nm and ~900 nm were observed for the 1 h and 10 h reaction times, respectively. The largest particle sizes were observed in ANO3 for the smallest amount of flux (1:1) and longest reaction time (10 h). While the individual $AgNbO_3$ particle sizes decreased both with increasing flux amounts and decreasing reaction times, a distribution of sizes could be found in all samples. For comparison, field-emission SEM images were taken of the $AgNbO_3$ sample prepared by the traditional solid-state method, as shown in Fig. 4. The solid-state products were observed to have no distinctly well-defined morphologies and exhibited a significantly wider range of particle sizes.

An EDX analysis was also performed on $AgNbO_3$ samples in order to confirm the elemental compositions, provided in the Supporting Information. The spectra revealed primarily Ag, Nb, and O in approximately the 1:1:3 molar ratio. Also, a small but detectable amount of Na was observed in all flux-prepared samples, indicating a small amount of incorporation of Na^+ from the Na_2SO_4 salt flux. The molar amount ranged from ~7% Na^+ for the 1:1 flux-prepared samples up to ~12% for the 3:1 flux-prepared samples. These represent the lowest and highest amounts of Na content from among all flux-prepared samples. As described in the PXRD data above, higher flux amounts or longer reaction times yield a minor impurity of $NaNbO_3$ in the products. $NaNbO_3$ is a known photocatalyst that is active in UV light only. No detectable amount of S was observed in any of the samples, indicating that the flux itself had been completely removed by the washing.

Surface area measurements were performed on each powdered $AgNbO_3$ sample, and these data are listed in Table 1. The largest measured surface area of 0.65 $m^2\ g^{-1}$ (ANO7) was obtained for the largest flux amount (3:1) and shortest reaction time (1 h), and conversely, the smallest surface area of 0.24 $m^2\ g^{-1}$ (ANO3) for the smallest flux amount (1:1) and longest reaction time (10 h). For intermediate flux reaction conditions, the surface area decreases in a regular way with increasing reactions times and decreasing flux-to-reactant ratios. This trend is consistent with the particle sizes calculated from the SEM images. Further, both the BET surface areas and SEM images confirm that reaction times have a more significant effect on the resulting $AgNbO_3$ particle sizes than the amount of flux used in the reaction. By comparison, the $AgNbO_3$ product prepared by the solid-state method exhibited a surface area of 0.55 $m^2\ g^{-1}$, and which is intermediate between that for the 1 h and 2 h flux reactions. The effects of slower cooling rates on the $AgNbO_3$ particles were also tested using a 1:1 flux-to-reactant ratio. The flux reactions were slow cooled from 900 °C to 750 °C at rates of 15 °C/h and 3 °C/h, while a third reaction was quickly radiatively cooled to room temperature in 0 h. The measured surface areas of the 0 h, 10 h, and 50 h cooled reactions gradually decreased from 0.39 $m^2\ g^{-1}$ to 0.30 $m^2\ g^{-1}$ and to 0.16 $m^2\ g^{-1}$, respectively. Therefore, the $AgNbO_3$ surface areas can also be controlled via tuning the cooling rate of the reaction, but not any more significantly than using the flux-to-reactant molar ratio or the reaction time.

3.2. Optical properties and photocatalytic activities

Measurements of the UV–vis diffuse reflectance spectra were taken on all $AgNbO_3$ samples in order to determine their optical bandgap sizes, and are shown for several selected samples in Fig. 5. In all cases, the bandgap sizes were calculated to be within a range of ~2.75–2.81 eV, consistent with previous reports [17]. However, the flux-prepared samples are slightly blue-shifted compared to the $AgNbO_3$ sample prepared by the solid-state method, most likely owing to the incorporation of small amounts of Na^+ into the products.

Using a traditional solid-state preparation, the $AgNbO_3$ particles have previously been shown to oxidize water to O_2 under visible-light irradiation, and with the aid of a cocatalyst, to reduce water

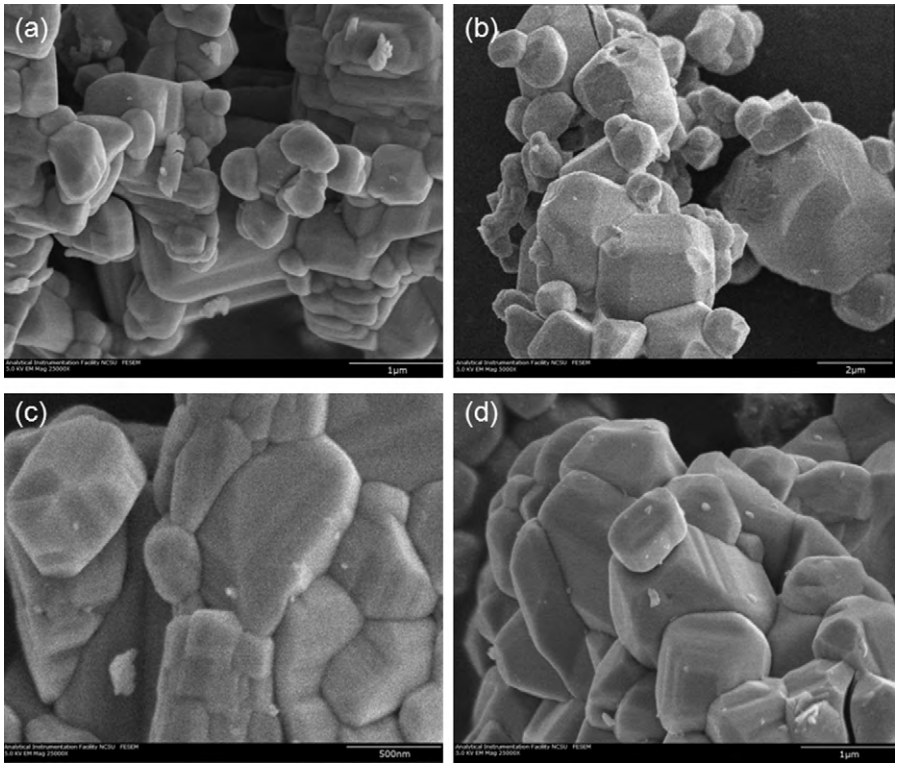

Fig. 3. Field-emission SEM images of flux-prepared $AgNbO_3$ particles using (a) 1:1 flux ratio at 1 h (ANO1), (b) 1:1 flux ratio at 10 h (ANO3), (c) 3:1 flux ratio at 1 h (ANO7), and (d) 3:1 flux ratio at 10 h (ANO9).

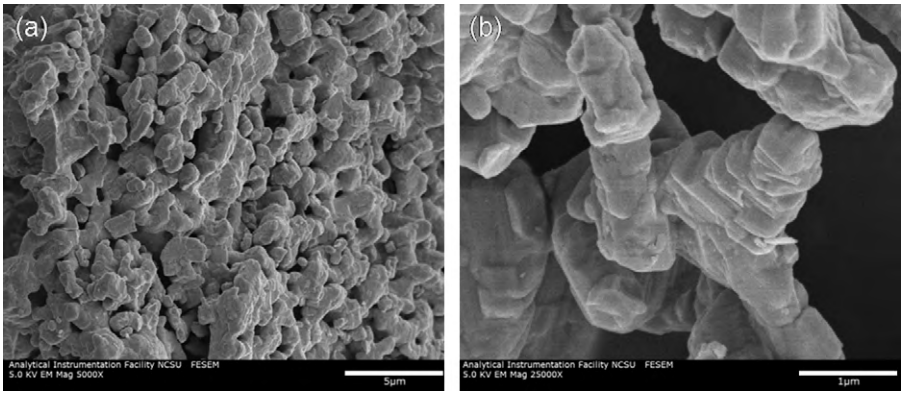

Fig. 4. Field-emission SEM images of a $AgNbO_3$ sample prepared by the solid-state method at 900 °C for 12 h.

Table 1
Measured BET surface areas, and visible-light (>420 nm) photocatalytic rates of H_2 formation,[a] for $AgNbO_3$ particles prepared using different flux conditions and also by the solid-state method.[b,c].

Sample ID	Flux:$AgNbO_3$ molar ratio	Reaction time (h)	Surface area ($m^2\ g^{-1}$)	Activity ($\mu mol\ H_2\ g^{-1}\ h^{-1}$)
ANO7	3:1	1	0.65	5.9
ANO4	2:1	1	0.61	1.7
ANO1	1:1	1	0.59	4.9
S.S. Method	–	12	0.55	3.5
ANO8	3:1	2	0.55	3.4
ANO5	2:1	2	0.54	2.5
ANO2	1:1	2	0.46	3.6
ANO9	3:1	10	0.43	2.7
ANO6	2:1	10	0.35	4.0
ANO3	1:1	10	0.24	2.4

[a] Photocatalysis conditions: 400 W Xe arc-lamp with 420 nm cutoff filter, 250 mg of $AgNbO_3$, 20% aqueous methanol solution, and 1 wt% Pt surface cocatalyst.
[b] Prepared by the solid-state reaction of Ag_2O and Nb_2O_5 at 900 °C for 12 h.
[c] All samples were radiatively cooled to room temperature at the time of reaction termination.

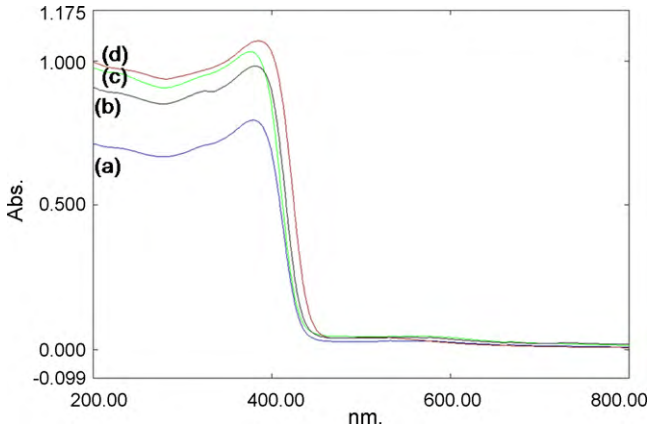

Fig. 5. Experimental UV–vis DRS data for flux-prepared $AgNbO_3$ using (a) 2:1 flux ratio at 10 h (ANO6), (b) 1:1 flux ratio at 10 h (ANO3), (c) 3:1 flux ratio at 10 h (ANO9), and (d) prepared using the solid-state method.

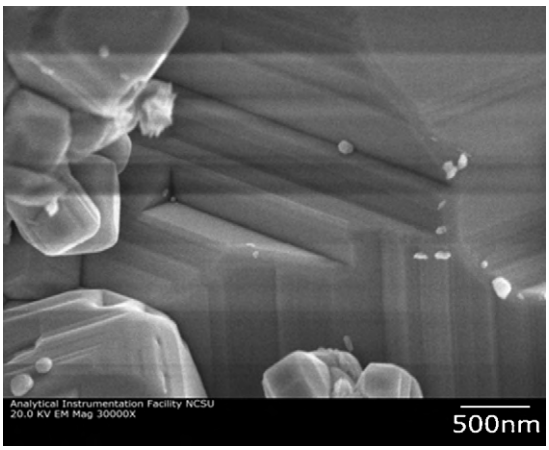

Fig. 7. Field-emission SEM images of post photocatalysis-tested surfaces of the solid-state prepared $AgNbO_3$ sample.

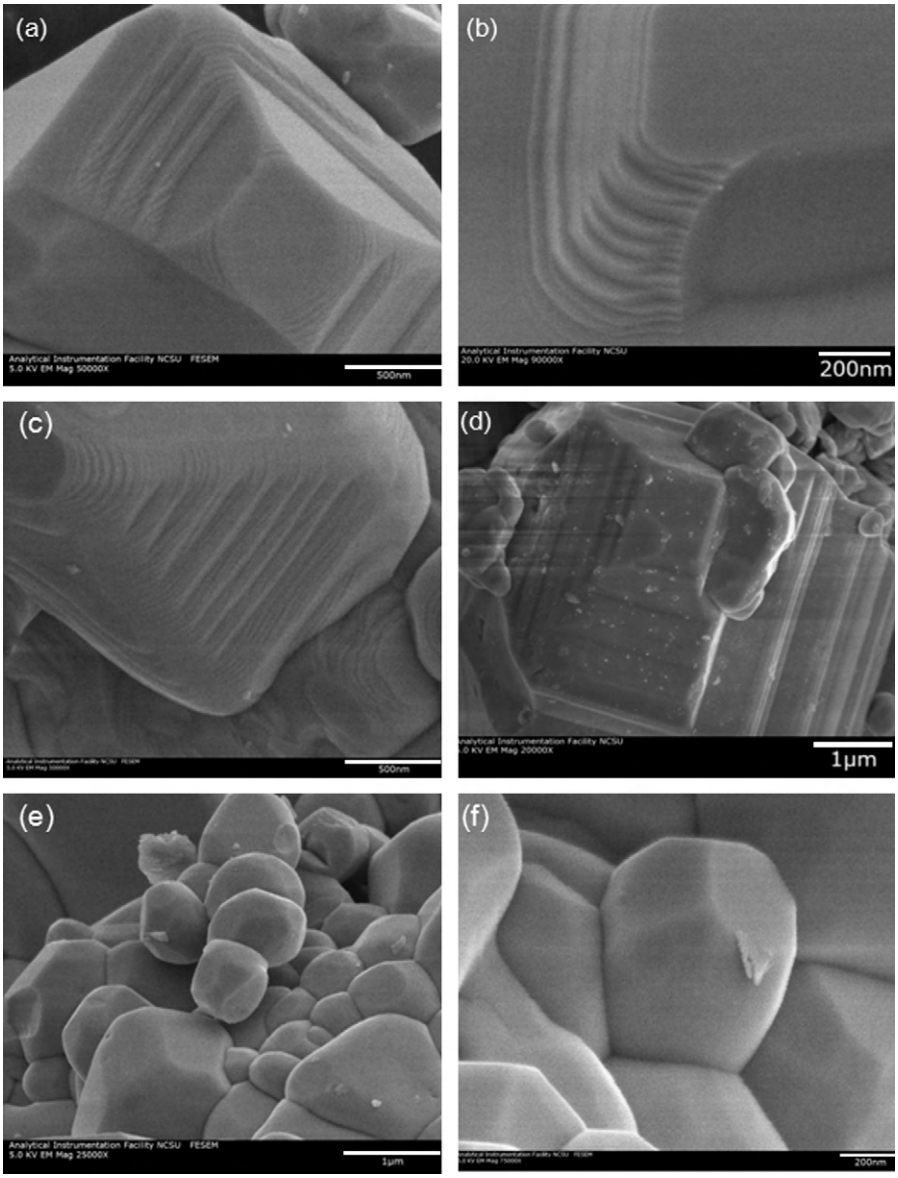

Fig. 6. High-magnification field-emission SEM images of flux-prepared $AgNbO_3$ particles using (a) 1:1 flux ratio at 10 h (ANO3), (b) 1:1 flux at 1 h (ANO1) showing ~20 nm stepped surface features, (c, d) 3:1 flux ratio at 1 h (ANO7), and (e, f) 2:1 flux ratio at 10 h (ANO6) that shows smooth surfaces.

to H_2 at rates of ~1.5 μmol H_2 g^{-1} h^{-1} in a 10% aqueous methanol solution [17]. When irradiated by photons of bandgap and greater energies, the electrons excited into the conduction band drive the reduction half reaction, while the remaining holes in the valence band are scavenged by methanol to produce CO_2. The latter is used in order to measure the formation rate of H_2 alone, as the oxidation of water to O_2 can be slower and rate limiting. Flux syntheses of different particle-size distributions should impact the rates of these surface reactions. The visible-light photocatalytic rates of H_2 formation for the flux-prepared $AgNbO_3$ products were measured and are listed in Table 1. For the 1:1 and 3:1 flux-to-reactant molar ratios, the rates of H_2 formation generally increased with higher surface areas and smaller particle sizes, as obtained by increasing the amount of flux and decreasing the reaction time. The highest observed rate of activity was 5.9 μmol H_2 g^{-1} h^{-1} for the $AgNbO_3$ particles prepared from the 3:1 flux-to-reactant ratio and heated for 1 h (ANO7). By contrast, for the 2:1 flux-prepared $AgNbO_3$ particles, the photocatalytic rates decreased with the shorter reaction times, and instead yielded the highest rate of 4.0 μmol H_2 g^{-1} h^{-1} for the longer 10 h reaction time (ANO6). For comparison, the photocatalytic rate of the solid-state prepared $AgNbO_3$ was measured to be 3.5 μmol H_2 g^{-1} h^{-1}. These results suggest that particle sizes and surface areas alone do not entirely determine the rate of photocatalysis.

Though particle size, in general, has been shown above to have an impact on the $AgNbO_3$ photocatalytic activity and rates, another critical consideration is the relative concentration of particle surfaces that are active versus inactive. As described above for $AgNbO_3$, and as described previously in studies on $La_2Ti_2O_7$ [31], the smaller particles generally exhibit the highest photocatalytic rates for H_2 formation. However, the 2:1 flux-prepared samples (ANO4, ANO5, ANO6) did not follow this expected behavior, listed in Table 1. Thus, higher-magnification field-emission SEM was used to further probe the surfaces of the $AgNbO_3$ particles exhibiting either the higher or lower activity rates. The SEM images, shown in Fig. 6, revealed a large concentration of nano-stepped terraced surfaces (20-50 nm) on the $AgNbO_3$ particles prepared with a 1:1 flux ratio at either 1 h (Fig. 6B) or 10 h (Fig. 6A). These nano-stepped features were also observed in the 3:1 flux-prepared samples, Fig. 6C and D, but in fewer numbers per particle. By contrast, the 2:1 flux-prepared sample (ANO6), shown in Fig. 6E and F, did not exhibit these nano-stepped surfaces, but however, exhibited the lowest rates of H_2 formation. Generally, the photocatalytic rates of $AgNbO_3$ particles with these surface nanosteps were among the highest observed, while samples that did not exhibit these features were much less active. The $AgNbO_3$ sample prepared by the solid-state method exhibited very irregular particle surfaces and no distinct and well-formed surface features. After ~6 h of photocatalysis testing, relatively larger and apparently etched edges of ~100–200 nm in size were also observed, shown in Fig. 7. The most inactive solid-state and flux-prepared $AgNbO_3$ samples frequently required a 1–2 h incubation period before any measurable activity began, and which may be the result of the time required for significant surface etching to occur. However, the PXRD patterns of the $AgNbO_3$ powders after phototesting showed no detectable degradation or photocorrosion yet, and the sample weights were approximately unchanged. A related study on the UV-photocatalyst $NaTaO_3$ shows that La-doping yields nano-stepped surface features similar to those found here, but at larger ~100–700 nm sizes [34,35]. These nanosteps at the metal-oxide surfaces are reported to create separate surface sites for the formation of H_2 and O_2 and also help to inhibit recombination. Therefore, it is likely that the nano-stepped features in $AgNbO_3$ have a similar effect. A recent report on the solvothermal synthesis of $AgNbO_3$ particles shows increased photocatalytic activity for O_2 formation [36], and that was associated with similar nano-stepped surfaces. Future *in situ* measurements are necessary to more deeply probe the origins and mechanisms of the active sites on the $AgNbO_3$ surfaces.

4. Conclusions

The synthesis of $AgNbO_3$ particles can be performed in a molten Na_2SO_4 flux at 900 °C in short reaction times of 1–10 h, with high purities and homogeneous microstructures that range in size from ~100 nm to 5000 nm. The smallest particle-size distributions of ~100–700 nm and highest surface areas of 0.65 m^2 g^{-1} were obtained for the largest amount of flux (3:1) and shortest reaction time (1 h). Measured optical bandgap sizes of the $AgNbO_3$ products were in the range of ~2.75–2.81 eV. Visible-light photocatalytic rates of the flux-synthesized $AgNbO_3$ particles for H_2 formation in an aqueous methanol solution were 1.7–5.2 μmol H_2 h^{-1} g^{-1}. The higher rates were correlated with the formation of ~20–50 nm terraced surface features on the flux-synthesized particles. By comparison, the $AgNbO_3$ sample prepared by solid-state methods showed no well-defined particle morphology or microstructure. Thus, the results herein demonstrate the value of flux-synthetic methods in tuning particle sizes and surface microstructures in order to probe the origins of photocatalytic activity on the surfaces of metal-oxide particles.

Acknowledgments

Financial support of this research is acknowledged from the Chemical Sciences, Geosciences and Biosciences Division, Office of Basic Energy Sciences, Office of Science, U.S. Department of Energy (DE-FG02-07ER15914).

Appendix A. Supplementary data

Supplementary data associated with this article can be found, in the online version, at doi:10.1016/j.jphotochem.2010.06.006.

References

[1] K. Domen, Bull. Chem. Soc. Jpn. 73 (2000) 1307.
[2] F.E. Osterloh, Chem. Mater. 20 (2008) 35.
[3] H. Kato, Catal. Today 78 (2003) 561.
[4] M.E. Graetzel, Energy Resources Through Photochemistry and Catalysis, Academic Press, New York, NY, 1983.
[5] H. Kato, K. Asakura, A. Kudo, J. Am. Chem. Soc. 125 (2003) 3082.
[6] D.W.H. Hyun, G. Kim, Chem. Commun. 12 (1999) 1077.
[7] A. Kudo, J. Phys. Chem. B 104 (2000) 571.
[8] G.H. Kim, Catal. Lett. 91 (2003) 193.
[9] A.K.S. Nakagawa, H. Kato, Chem. Lett. 11 (1999) 1197.
[10] R. Abe, M. Higashi, K. Sayama, Y. Abe, H. Sugihara, J. Phys. Chem. B 110 (2006) 2219.
[11] T.R.N. Kutty, M. Avudaithai, Catal. Rev. 34 (1992) 373.
[12] M. Machida, J.-I. Yabunaka, T. Kijima, Chem. Commun. 19 (1999) 1939.
[13] M. Machida, K. Miyazaki, S. Matsushima, M. Arai, J. Mater. Chem. 13 (2003) 1433.
[14] T. Takata, J. Photochem. Photobiol. A: Chem. 106 (1997) 45.
[15] K. Domen, Catal. Lett. 4 (1990) 339.
[16] K.-I. Shimizu, Y. Tsuji, T. Hatamachi, K. Toda, T. Kodama, M. Sato, Y. Kitayama, Phys. Chem. Chem. Phys. 6 (2004) 1064.
[17] H. Kato, N. Matsudo, H. Kobayashi, A. Kudo, J. Phys. Chem. B 106 (2002) 12441.
[18] H. Kato, N. Matsudo, A. Kudo, Chem. Lett. 33 (2004) 1216.
[19] R. Konta, H. Kato, H. Kobayashi, A. Kudo, Phys. Chem. Chem. Phys. 5 (2003) 3061.
[20] C. Chiu, C. Li, S.B. Desu, J. Am. Ceram. Soc. 74 (1991) 38.
[21] R.H. Arendt, J. Solid State Chem. 8 (1973) 339.
[22] R.H. Arendt, J.H. Rosolowski, J.W. Szymaszek, Mater. Res. Bull. 14 (1979) 703.
[23] D.B. Hedden, J. Solid State Chem. 118 (1995) 419.
[24] M.A. El-Toni, Mater. Lett. 60 (2006) 185.
[25] Y. Kan, Cryst. Eng. 38 (2003) 567.
[26] M. Lukaszewski, A. Kania, A. Ratuszna, J. Cryst. Growth 48 (1980) 493.
[27] J. Fabry, Z. Zikmund, A. Kania, V. Petricek, Acta Crystallogr. C 56 (2000) 916.
[28] D. Schwartzenbach, Acta Crystallogr. A 45 (1989) 63.
[29] H. Nakamatsu, J. Chem. Soc., Faraday Trans. I 82 (1985) 527.
[30] D.G. Porob, P.A. Maggard, J. Solid State Chem. 179 (2006) 1727.

[31] D. Arney, B. Porter, B. Greve, P.A. Maggard, J. Photochem. Photobiol. A: Chem. 199 (2008) 230.
[32] D.G. Porob, P.A. Maggard, Mater. Res. Bull. 41 (2006) 1513.
[33] D.G. Porob, P.A. Maggard, Chem. Mater. 19 (2007) 970.
[34] A. Kudo, Chem. Phys. Lett. 331 (2000) 373.
[35] A.A. Kudo, Chem. Lett. 33 (2004) 1534.
[36] G. Li, S. Yan, Z. Wang, X. Wang, Z. Li, J. Ye, Z. Zou, Dalton Trans. 40 (2009) 8519.